Lasers in Surgery and Medicine 38:754–761 (2006)

# Feasibility of Interstitial Doppler Optical Coherence Tomography for *In Vivo* Detection of Microvascular Changes During Photodynamic Therapy

**Heng Li,[1†] Beau A. Standish,[1†] Adrian Mariampillai,[1] Nigel R. Munce,[1] Youxin Mao,[1] Stephanie Chiu,[1] Norman E. Marcon,[2] Brian C. Wilson,[1,3] Alex Vitkin,[1,3,4] and Victor X.D. Yang[3]***

[1]*Department of Medical Biophysics, University of Toronto, Toronto, Ontario, Canada*
[2]*Therapeutic Endoscopy Center, St. Michael's Hospital, Toronto, Ontario, Canada*
[3]*Ontario Cancer Institute / University Health Network, Toronto, Ontario, Canada*
[4]*Department of Radiation Oncology, University of Toronto, Toronto, Ontario, Canada*

**Introduction:** Doppler optical coherence tomography (DOCT) is an emerging imaging modality that provides subsurface microstructural and microvascular tissue images with near histological resolution and sub-mm/second velocity sensitivity. A key drawback of OCT for some applications is its shallow (1–3 mm) penetration depth. This fundamentally limits DOCT imaging to transparent, near-surface, intravascular, or intracavitary anatomical sites. Consequently, interstitial Doppler OCT (IS-DOCT) was developed for minimally-invasive in vivo imaging of microvasculature and microstructure at greater depths, providing access to deep-seated solid organs. Using Dunning prostate cancer in a rat xenograft model, this study evaluated the feasibility of IS-DOCT monitoring of microvascular changes deep within a tumor caused by photodynamic therapy (PDT).

**Materials and Methods:** The DOCT interstitial probe was constructed using a 22 G (diameter ~0.7 mm) needle, with an echogenic surface finish for enhanced ultrasound visualization. The lens of the probe consisted of a gradient-index fiber, fusion spliced to an angle-polished coreless tip to allow side-view scanning. The lens was then fusion spliced to a single-mode optical fiber that was attached to the linear scanner via catheters and driven along the longitudinal axis of the needle to produce a 2D subsurface DOCT image. The resultant IS-DOCT system was used to monitor microvascular changes deep within the tumor mass in response to PDT in the rat xenograft model of Dunning prostate cancer. Surface PDT was delivered at 635 nm with 40 mW of power, for a total light dose of 76 J/cm$^2$, using 12.5 mg/kg of Photofrin as the photosensitizer dose.

**Results:** IS-DOCT demonstrated its ability to detect microvasculature *in vivo* and record PDT-induced changes. A reduction of detected vascular cross sectional area *during* treatment and partial recovery *post*-treatment were observed.

**Conclusions:** IS-DOCT is a potentially effective tool for real-time visualization and monitoring of the progress of PDT treatments. This capability may play an important role in elucidating the mechanisms of PDT in tumors, pre-treatment planning, feedback control for treatment optimization, determining treatment endpoints and post-treatment assessments. Lasers Surg. Med. 38:754–761, 2006. © 2006 Wiley-Liss, Inc.

**Key words:** optical coherence tomography; photodynamic therapy; Doppler blood flow imaging; interstitial fiber sensors

## INTRODUCTION

Optical coherence tomography (OCT) [1] and its functional extension Doppler optical coherence tomography (DOCT) [2–4] are emerging tissue assessment tools that can provide near-histological microstructural and microvascular images, with flow sensitivities approaching a few micrometers per second [5–7]. DOCT combines the high-resolution structural imaging capability of OCT with Doppler detection of microvascular blood flow, and has demonstrated *in vivo* functional imaging in organs such as the retina [7,8], skin [9–12], and gastrointestinal tract [13,14]. However, many clinical applications require high-resolution imaging of deeply seated tissues, and these anatomical sites cannot be reached by conventional OCT due to its limited penetration depth of 1–3 mm in non-transparent tissues. Consequently, *in vivo* imaging of microvasculature using DOCT has been limited to transparent organs or near-surface applications such as epithelial layers of the GI tract. Needle-based interstitial Doppler OCT (IS-DOCT) has been described by us previously as a

[†]Heng Li and Beau A. Standish contributed equally to this work.

Contract grant sponsor: Canadian Institutes of Health Research; Contract grant sponsor: Photonics Research Ontario; Contract grant sponsor: Premier's Research Excellence Award; Contract grant sponsor: Gordon Lang Samuel B. McLaughlin Foundations; Contract grant sponsor: Canadian Cancer Society; Contract grant sponsor: National Cancer Institute of Canada.

*Correspondence to: Dr. Victor X.D. Yang, 610 University Ave, 7th floor, Toronto, Ont., Canada M5G2M9.
E-mail: victor.xd.yang@gmail.com

Accepted 2 July 2006
Published online 22 August 2006 in Wiley InterScience (www.interscience.wiley.com).
DOI 10.1002/lsm.20387

useful technique for in vivo assessment of microvasculature and microstructure at a greater depth, providing potential accessibility of DOCT to anatomical sites such as the brain, liver, pancreas, or prostate [15].

Photodynamic therapy (PDT) is an emerging treatment that causes cellular and/or vascular tissue damage through photoproducts (most often excited singlet-state oxygen) generated by light activation of photosensitizers. Tumor destruction is associated with PDT's ability to induce cellular apoptosis [16], activate the host immune system [17] and/or cause vascular damage [18], depending on the photosensitizer [19], the drug-light time interval which control the (micro) localization of the photosensitizer, and several tissue and host factors. PDT tissue damage is localized to zones where light, photosensitizer, and oxygen overlap to create a region with a high concentration of reactive oxygen species. Destruction of tumor microvasculature is frequently an important mechanism of PDT, in which damage to the endothelium cells of blood vessels causes increased vessel permeability, vasoconstriction, and thrombosis [20], resulting in localized vessel occlusion and tissue hypoxia [21]. Specifically, PDT of prostate cancer is in clinical trials using the direct vascular effects of a rapidly clearing photosensitizer [22]. Therefore, monitoring the vascular dynamics of PDT in real time could be useful in providing treatment feedback, potentially for real-time control, and for assessing and, ultimately, predicting treatment effectiveness. We hypothesize that IS-DOCT may be used in this way to monitor and quantify PDT-induced tumor vascular response deep within tissue for an accurate assessment of the degree and extent of vascular shutdown, which may predict the treatment's therapeutic efficacy. As a first step, in this study, we constructed a novel IS-DOCT probe and used it to investigate the feasibility of IS-DOCT to monitor the deep tumor vascular response to PDT in Dunning prostate cancer xenografts.

## MATERIALS AND METHODS

### IS-DOCT Probe and System

The design and configuration of the time-domain DOCT system used in this study have been described previously [6]. Briefly, this system utilizes a near-infrared source at 1.3 μm center wavelength, with a coherence length of 10 μm in tissue and a Doppler flow sensitivity of ~0.02 mm/second at 1 frame per second (fps). Figure 1 shows a schematic of the system. Tissue reflectivity, color Doppler and velocity variance are computed and displayed simultaneously.

To date, reported needle probe designs include radial-sector-scanning by Li et al. [23], ball-lens systems by Yang et al. [15], Boppart et al. [24] and Shishkov et al. [25], and gradient-index (GRIN) fibers by Reed et al. [26]. Our IS-DOCT needle probe (Fig. 2a) uses a 22 G echogenic needle (0.7 mm outer diameter) that is compatible with interventional radiological guidance, and is actuated by a linear scanner via flexible catheters. It is designed to be less invasive than our previously reported needle probe, which had a diameter of 0.9 mm [15]. The optics in the needle probe are similar to the design first demonstrated by Reed et al. [26]. The lens (Fig. 2b) consists of a 140 μm diameter clad and 100 μm diameter core multi-mode GRIN fiber fusion spliced to an unbuffered tip (8 cm) of a 125 μm diameter single-mode (SM) fiber. The GRIN fiber is manually cleaved at ~0.83 pitch (~1.38 mm), then

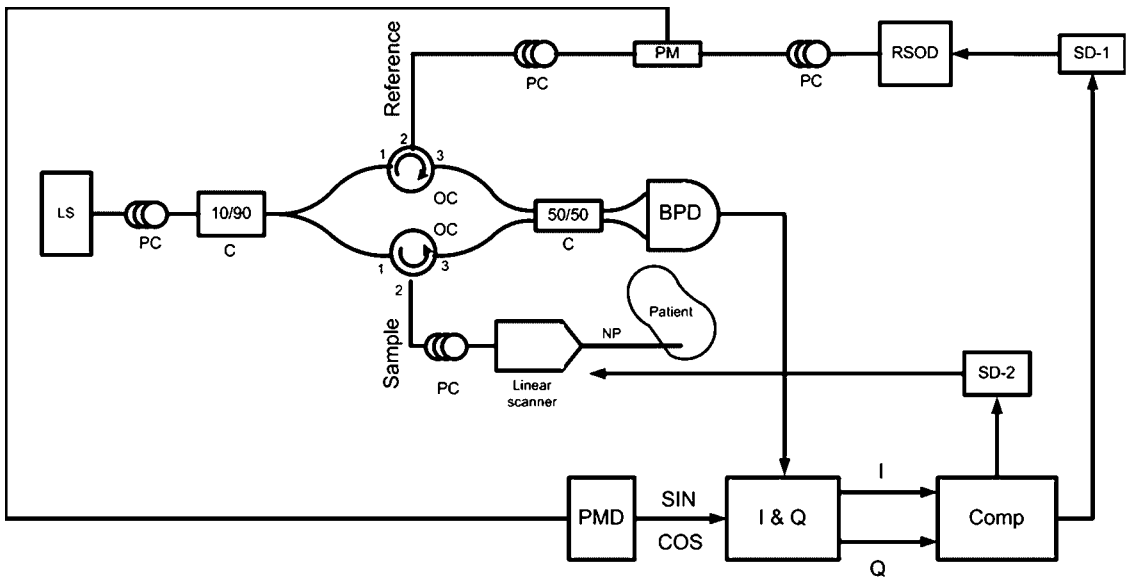


Fig. 1. Schematic diagram of the DOCT system. LS, light source; PC, polarization controller; C, coupler; OC, optical circulator; PM, RF phase modulator; RSOD, rapid scanning optical delay; SD 1 and 2, scan drivers; BPD, balanced photodetector; PMD, phase modulator driver; SIN & COS, 0 and 90 degree shifted carrier frequency; I & Q, inphase and quadrature signals; Comp, computer; NP, needle probe.

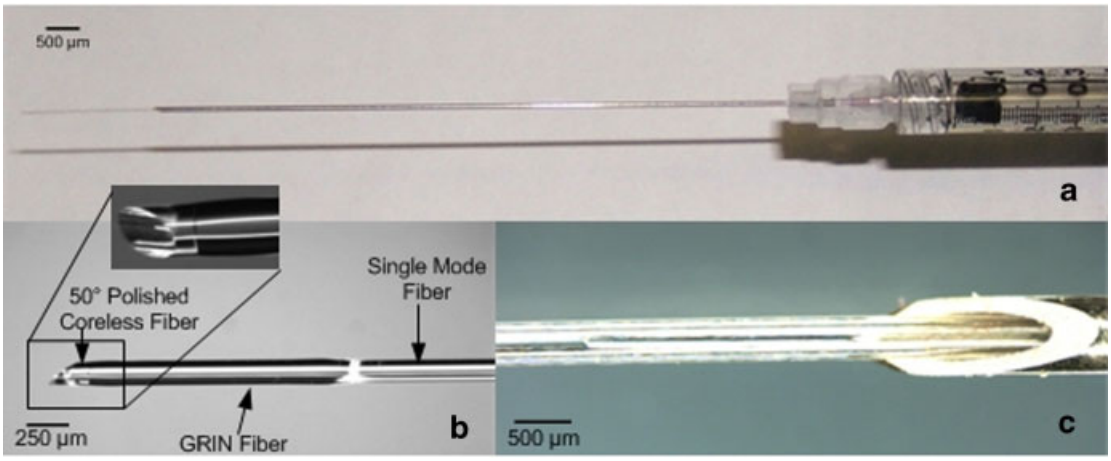


Fig. 2. IS-DOCT needle probe, showing the GRIN fiber fusion spliced to the angle-polished coreless fiber. **a**: IS-DOCT needle probe; (**b**) lens components: single mode fiber, GRIN fiber, and coreless tip; (**c**) retracted needle, exposing the lens, and protective tubing.

shortened to ~0.80 pitch (~1.32 mm) by polishing, to focus light at a distance of ~400 μm in air and ~286 μm in tissue ($n = 1.4$). The polished end of the GRIN fiber is then fusion spliced to an angle-polished, coreless fiber tip to allow total internal reflection.

The lens and the unbuffered portion of the SM fiber are protected in a transparent inner catheter (OD 394 m), with a maximum air gap of 2 μm between the fiber and the catheter to limit aberrations. The depth of field was measured to be 470 μm, corresponding to a spot size of 19.8 μm. The buffered portion of the fiber is attached to an outer catheter (OD 1.4 mm), which is fastened onto a modified 1 ml syringe piston, while the transparent inner catheter is inserted into a 22 G (0.7 mm), 8.89 cm long, echogenic spinal needle (VWR, Mississauga, ON, Canada). The inner catheter is 2–3 cm longer so that, after insertion into the tissue, the needle can be drawn back while the optical probe stays stationary (Fig. 2c). The probe is then driven axially inside the catheter by a linear scanner, such that a two dimensional DOCT image is formed in combination with the coherence depth scanning.

### Animal Models

This study used eight male Copenhagen rats (Charles River Laboratories, Wilmington, MA) housed in standard conditions under a protocol approved by the institutional animal care committee at St. Michael's Hospital, Toronto, Canada.

Mat-Ly-Lu rat prostate cancer cells were derived from the subline R3327-AT-1 rat prostate cells and were maintained as cell cultures in growth media (RPMI 1640 media+L-Glutamine, 10% fetal bovine serum, 1% penicillin and streptomycin). Five to ten percent of the cells were resuspended every other day to prevent overgrowth. Cells were harvested and prepared at $2\times10^6$ cells/ml for injection.

One animal was used to test the IS-DOCT ability to detect vasculature in normal tissue. In seven animals, intradermal bolus injections of 0.1 ml of the injectate were administered in the hind leg after removal of hair and sterilization of the skin. The tumor was grown for 10–14 days or to a diameter of 0.5–1 cm. Four of the tumor-bearing rats were injected with Photofrin® (Axcan Pharma, Mont-Saint-Hilaire, QC, Canada), while the other three were used as light-only controls.

All tumor-bearing animals underwent PDT-prescribed light exposures and were anaesthetized with isoflurane and oxygen at a 1:1 ratio through a nose cone. The rats were kept at body temperature during all experimental procedures. After imaging, the animals were euthanized.

### PDT Treatment and DOCT Imaging

Photofrin was injected via the tail vein 20–24 hours prior to treatments under isofluorane anesthesia. At 20–24 hours later, the tumor surface was irradiated superficially through the intact skin with a 635 nm diode laser (University Health Network, Laboratory of Applied Biophotonics, Toronto, ON, Canada) at 40 mW. The total light dose, delivered over 25 minutes via a 100 μm core (numerical aperture = 0.22) optical fiber collimated to a ~10 mm spot size, was ~76 J/cm$^2$.

IS-DOCT was used to collect structural, color Doppler and velocity variance images before, during and post-PDT treatment at an imaging rate of 1 fps. The interstitial probe was inserted under the tumor with the imaging direction toward the tumor bulk to detect peripheral microvasculature (Fig. 3). PDT treatment was started after small blood vessels were located using IS-DOCT. Imaging was continuous and divided into three imaging periods: before ($t = 0$–5 minutes), during ($t = 5$–30 minutes), and after ($t = 30$–40 minutes) treatment. The cross-sectional areas of the blood vessels were measured by pixel counts of the color-coded regions in the velocity variance images. These were then averaged for each minute during IS-DOCT treatment monitoring; we define this value as the vascular index. The vascular index for each minute of imaging was then

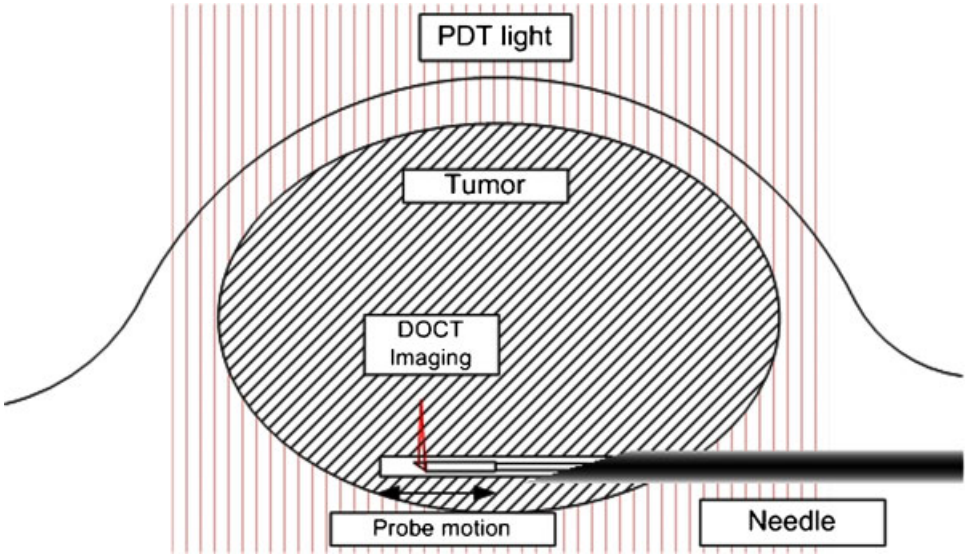


Fig. 3. Insertion of the needle probe near the base of the tumor, imaging in the direction shown.

normalized to the highest value throughout the treatment. The changes in detected blood flow could then be quantified by analyzing the normalized vascular index as a function of time before, during, and after PDT treatment.

## RESULTS

Xenograft tumors were successfully grown in seven rats, with diameters of 0.5–1 cm and 0.3–0.8 cm high. Neither treatment nor tumor-induced deaths occurred. Gross PDT responses, including erythema and edema, were observed in all four rats treated with Photofrin-PDT.

Initial IS-DOCT imaging of the non-tumor-bearing rat showed that deeply situated blood vessels could be readily detected. A typical image is shown in Figure 4, where a small branch of a deep femoral vessel was clearly visualized at a distance of $>\sim$400 μm from the interstitial probe tip.

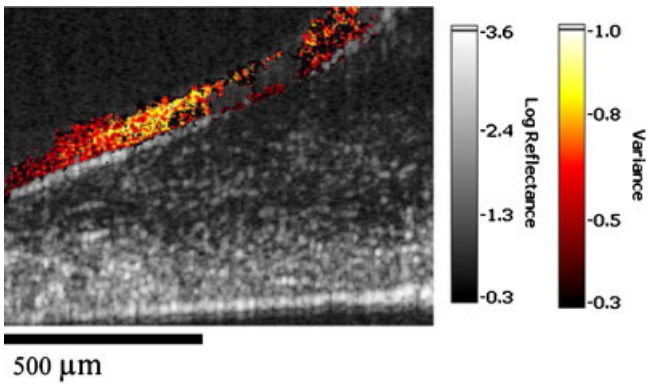


Fig. 4. IS-DOCT image of a small branch of a deep femoral vessel in normal muscle tissue at a distance of ~400 μm from the surface of the interstitial probe. The structural image is shown in gray-scale, while the velocity variance is shown in a false-color scale. [Figure can be viewed in color online via www.interscience.wiley.com.]

*In vivo* monitoring of PDT using IS-DOCT was performed in all tumor-bearing rats ($n = 4$ with Photofrin injection, $n = 3$ as light-only controls). Figure 5 shows an example of the detected vasculature presented in color Doppler (a) and velocity variance (b) images. A typical sequence of velocity variance images obtained in the course of the treatment (Fig. 6) demonstrated a pair of blood vessels that underwent complete vascular shutdown, with partial recovery in the right vessel post-treatment. Figure 7 shows the average change of normalized vascular index during PDT: significant changes in vascular index during and post-PDT were consistently observed, with an average decrease of 76% by the end of treatment. Individual rats exhibited decrease in the vascular index value during treatment; however, there were large inter-animal differences in the change of the vascular index. Controls ($n = 3$, light only) imaged during exposure to the same light dose (~76 J/cm$^2$) showed only slight changes in the vascular index during and after light exposure.

## DISCUSSION

PDT is an emerging treatment option for human cancers and other pathologies. It can be applied alone or in conjunction with other treatments [27,28]. It has been shown PDT can damage tumor cells and/or tumor microvasculature, the latter causing reduced blood flow or permanent vessel occlusion [18,20], which may aid in tumor eradication through hypoxia and nutrient deficiency [29]. However, significant vascular damage or irreversible occlusion during treatment may also diminish PDT efficacy, since the photodynamic process depends on the presence of both oxygen and photosensitizer, either of which may decrease during vascular shutdown [30]. Hence, measuring the microvascular response to PDT in different individualized patients may be important for planning and predicting treatment efficacy.

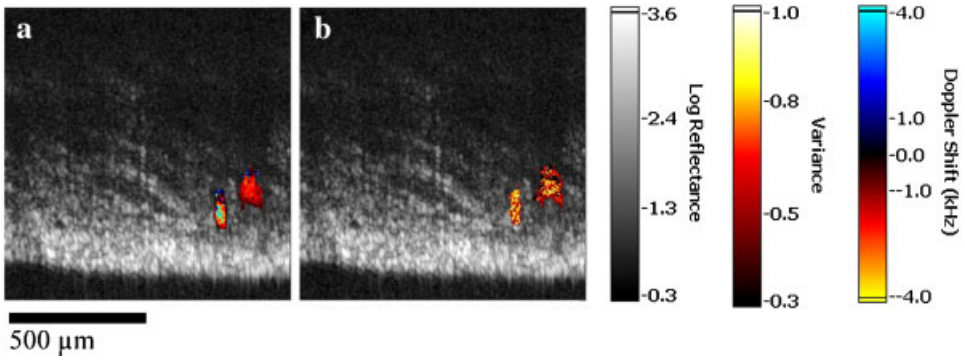


Fig. 5. IS-DOCT image showing (**a**) color Doppler and (**b**) velocity variance maps of detected blood vessels in tumor before PDT treatment. [Figure can be viewed in color online via www.interscience.wiley.com.]

In this study, we have demonstrated that IS-DOCT is technically feasible (a) to detect tumor microvasculature and (b) to quantitatively monitor and assess the vascular changes in response to PDT in deep tissue. It may be possible to differentiate an artery-vein vascular bundle through indicated flow directions and flow intensities in color Doppler images. A slight reduction of vascular index in the controls (light only, $n = 3$) was observed, possibly due to tissue trauma and slight blood pooling in the tumor, although not sufficient to disrupt the DOCT images. However, this requires further investigation. The reduction in vascular index in tumor due to PDT showed similar trends as observed in our previous studies in normal rat colon and Dunning prostate models [31]. Previously, Wang et al. [32] demonstrated that changes in tumor oxygenation correlated to the therapeutic outcome of PDT. IS-DOCT may complement these correlations through direct measurements of the microvascular response to PDT. Although changes in the blood flow *during* PDT light irradiation was quantified by the DOCT data, questions are raised about how this data will be used to predict treatment response and outcome. Rapid vascular responses during PDT have been noted by other authors, for example by Wiemen et al. [33] who used laser Doppler velocimetry to

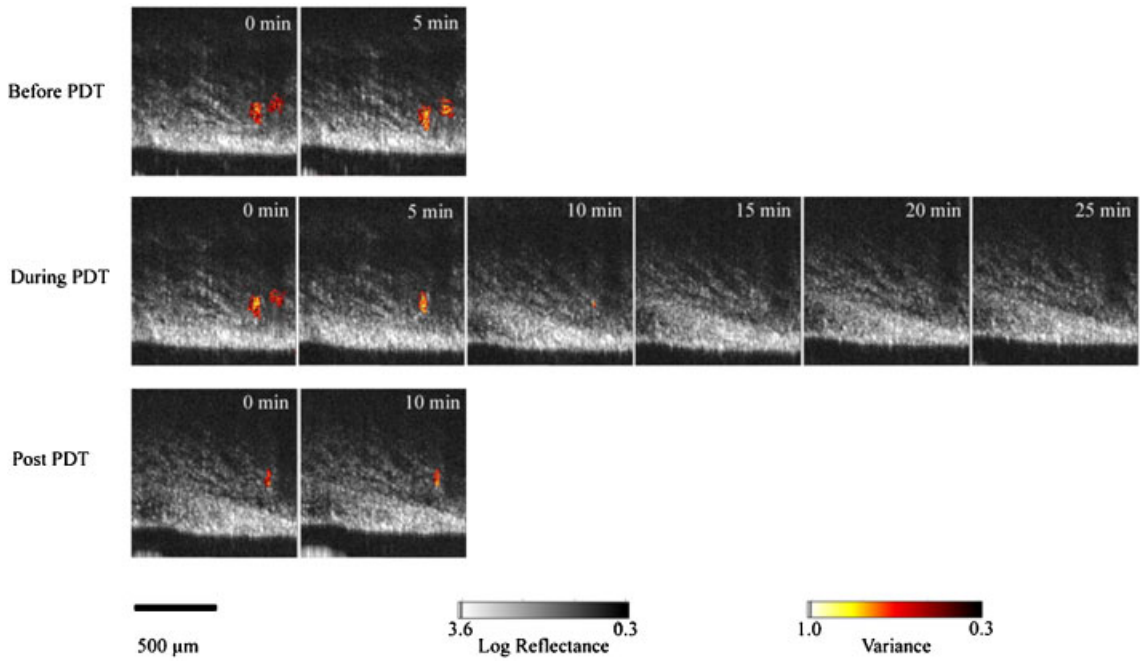


Fig. 6. Comparison of IS-DOCT images of a Dunning prostate tumor before (5 minutes) during (25 minutes), and after (10 minutes) PDT light exposure for a total imaging time of 40 minutes. Blood flow is color-coded by the detected velocity variance images. A noticeable reduction in vessel cross sectional area was seen during treatment and slight vascular recovery occurred post-treatment. The blood vessel on the left shutdown first and recovery was not detected. [Figure can be viewed in color online via www.interscience.wiley.com.]

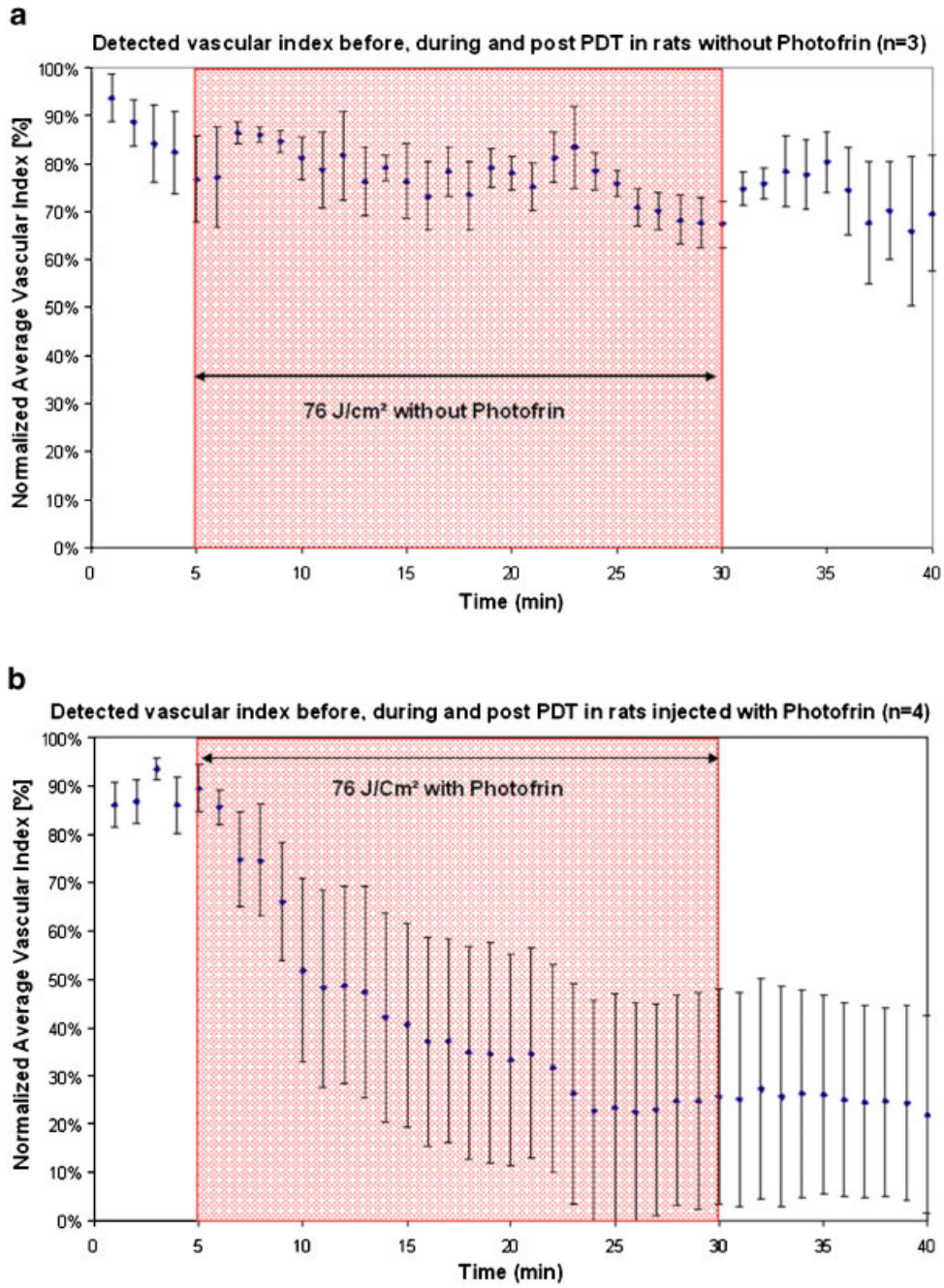


Fig. 7. Normalized average vascular index in tumor (**a**) without Photofrin and (**b**) with Photofrin before, during, and after light treatment, showing minimal response in the light-only controls and large vascular response in the PDT group, respectively. The error bars correspond to standard error between animals.

measure Photofrin-PDT induced changes in single arterioles in SMT-F mammary tumors and observed a prompt blood flow reduction that was photosensitizer and light dose dependent, at least within certain dose ranges. This marked change occurred after delivery of only a fraction of the total light dose, as we have observed also in other tumor models [31] and the effect is photosensitizer- and tissue-dependent.

The dynamic changes and observed results emphasized the fact that PDT is a dynamic and complex process, in which the tissue response is often variable, so that accurate, real-time assessment of treatment delivery and therapeutic response is important but very challenging. In order to elucidate further the mechanisms of PDT using IS-DOCT and to use IS-DOCT data as a predictive measure, it will be important to determine the relationships between

PDT and the microvascular response as measured by IS-DOCT. It may be that different IS-DOCT blood flow metrics will be required for different applications (target tissues, photosensitizers, and mechanisms of action). With Photofrin, for example, there is known to be both a vascular and direct cell effect in the tumor response [31], while blood flow measurements would monitor only the former. However, with vascular-targeted photosensitizers such as TOOKAD™ [21], the DOCT changes should be more tightly predictive of tissue damage and, hence, of outcome.

Future investigations will include larger sample sizes to evaluate the correlation between vascular shutdown and PDT parameters. Comparisons of IS-DOCT results to other measures of microvascular responses also need to be made, for example, under tumor manipulation of tumor oxygenation during PDT, while 3D volumetric perfusion measurements of the PDT-induced vascular responses may provide better measurement accuracy.

In conclusion, IS-DOCT may be an effective tool for high-resolution, real-time visualization, and monitoring of the tissue microvascular response of PDT. This capability may play an important role in pre-treatment planning, feedback control for treatment optimization, determining treatment endpoints and post-treatment assessment.

## ACKNOWLEDGMENTS

This work was supported by the Canadian Institutes of Health Research, Photonics Research Ontario, the Premier's Research Excellence Award, the Gordon Lang Samuel B. McLaughlin Foundations, and the Canadian Cancer Society through a grant from the National Cancer Institute of Canada. The authors acknowledge assistance from Drs. Annie Lin, Anoja Giles, and Dr. Margarete Akens from the Ontario Cancer Institute, Toronto, ON, Canada.

## REFERENCES

1. Huang D, Swanson EA, Lin CP, Schuman JS, Stinson WG, Chang W, Hee MR, Flotte T, Gregory K, Puliafito CA, Fujimoto JG. Optical coherence tomography. Science 1991; 254:1178–1181.
2. Wang XJ, Milner TE, Nelson JS. Characterization of fluid flow velocity by optical Doppler tomography. Opt Lett 1995;20:1337–1339.
3. Izatt JA, Kulkarni MD, Yazdanfar S, Barton JK, Welch AJ. In vivo bidirectional color Doppler flow imaging of picoliter blood volumes using optical coherence tomography. Opt Lett 1997;22:1439–1441.
4. Chen Z, Milner TE, Digant D, Nelson SJ. Optical Doppler tomographic imaging of fluid flow velocity in highly scattering media. Opt Lett 1997a;22:64–66.
5. Yazdanfar S, Rollins AM, Izatt JA. Ultrahigh velocity resolution imaging of the microcirculation in vivo using color Doppler optical coherence tomography. Proc SPIE 2001;4251: 156–164.
6. Yang VXD, Gordon ML, Qi B, Pekar J, Lo S, Seng-Yue E, Mok A, Wilson BC, Vitkin IA. High speed, wide velocity dynamic range Doppler optical coherence tomography (Part I): System design, signal processing, and performance. Opt Express 2003;11:794–809.
7. White BR, Pierce MC, Nassif N, Cense B, Park BH, Tearney GJ, Bouma BE, Chen TC, de Boer JF. In vivo dynamic human retinal blood flow imaging using ultra-high-speed spectral domain optical coherence tomography. Opt Express 2003;11: 3490–3497.
8. Yazdanfar S, Rollins AM, Izatt JA. Imaging and velocimetry of the human retinal circulation with color Doppler optical coherence tomography. Opt Lett 2000;25:1448–1450.
9. Nelson JS, Kelly KM, Zhao YH, Chen ZP. Imaging blood flow in human port-wine stain in situ and in real time using optical Doppler tomography. Arch Dermatol 2001;137: 741–744.
10. Zhao YH, Chen ZP, Saxer C, Xiang SH, de Boer JF, Nelson JS. Phase-resolved optical coherence tomography and optical Doppler tomography for imaging blood flow in human skin with fast scanning speed and high velocity sensitivity. Opt Lett 2000;25:114–116.
11. Tang SJ, Gordon ML, Yang VXD, Faughnan ME, Cirocco M, Qi B, Yue ES, Gardiner G, Haber GB, Kandel G, Kortan P, Vitkin A, Wilson BC, Marcon NE. In vivo Doppler optical coherence tomography of mucocutaneous telangiectases in hereditary hemorrhagic telangiectasia. Gastrointest Endosc 2003;58:591–598.
12. Zhao Y, Chen ZP, Saxer C, Shen Q, Xiang S, de Boer JF, Nelson JS. Doppler standard deviation imaging for clinical monitoring of in vivo human skin blood flow. Opt Lett 2000; 25:1358–1360.
13. Yang VXD, Gordon ML, Tang SJ, Marcon NE, Gardiner G, Qi B, Bisland S, Seng-Yue E, Lo S, Pekar J, Wilson BC, Vitkin IA. High speed, wide velocity dynamic range Doppler optical coherence tomography (part III): In vivo endoscopic imaging of blood flow in the rat and human gastrointestinal tract. Opt Express 2003c;11:2416–2424.
14. Yang VXD, Tang SJ, Gordon ML, Qi B, Gardinar G, Kortan P, Haber GB, Kandel G, Vitkin IA, Wilson BC, Marcon NE. Endoscopic Doppler optical coherence tomography: First clinical experience with a novel imaging technique. Gastrointest Endosc 2005;61:879–890.
15. Yang VXD, Mao YX, Munce N, Standish B, Kucharczyk W, Marcon NE, Wilson BC, Vitkin IA. Interstitial Doppler optical coherence tomography. Opt Lett 2005a;30:1791–1793.
16. Oleinick NL, Morris RL, Belichenko I. The role of apoptosis in response to photodynamic therapy: What where, why, and how. Photochem Photobiol Sci 2002;1:1–21.
17. Van Duijnhoven FH, Aalvers RI, Rovers JP, Terpstra OT, Kuppen PF. The immunological consequences of photodynamic treatment of cancer, a literature review. Immunobiology 2003;207:105–113.
18. Chen B, Pogue BW, Goodwin IA, O'Hara JA, Wilmot CM, Hutchins JE, Hoopes PJ, Hasan T. Blood flow dynamics after photodynamic therapy with verteporfin in the RIF-1 tumor. Radiat Res 2003;160:452–459.
19. Lilge L, Portnoy M, Wilson BC. Apoptosis induced in vivo by photodynamic therapy in normal brain and intracranial tumour tissue. Br J Cancer 2000;83(8):1110–1117.
20. Fingar V, Wieman T, Wiehle S, Cerrito P. The role of microvascular damage in photodynamic therapy: The effect of treatment on vessel constriction, permeability, and leukocyte adhesion. Cancer Res 1992;52:4914–4921.
21. Busch TM, Hahn SM, Evans SM, Koch CJ. Depletion of tumor oxygenation during photodynamic therapy: Detection by the hypoxia marker EF3 [2-(2-nitroimidazol-1[H]-yl)-N-(3,3,3-trifluoropropyl)acetamide]. Cancer Res 2000;60:2636–2642.
22. Weersink RA, Bogaards A, Gertner M, Davidson SRH, Zhang K, Netchev G, Trachtenberg J, Wilson BC. Techniques for delivery and monitoring of TOOKAD (WST09)-mediated photodynamic therapy of the prostate: Clinical experience and practicalities. Photochem Photobiol 2005;79:211–222.
23. Li X, Chudoba C, Ko T, Pitris C, Fujimoto JG. Imaging needle for optical coherence tomography. Opt Lett 2000;25:1520–1522.
24. Boppart SA, Luo W, Marks DL, Singletary KW. Optical coherence tomography: Feasibility for basic research and image-guided surgery of breast cancer. Breast Cancer Res Treat 2004;84:85–97.
25. Shishkov M, Tearney GJ, Bouma BE. Sculptured optical fiber tips for narrow diameter optical catheters. OSA Biomedical

Topical Meeting (Optical Society of America; 2004. paper SE5).
26. Reed WA, Yan MF, Schnitzer MJ. Gradient-index fiber-optic microprobes or minimally invasive in vivo low-coherence interferometry. Opt Lett 2002;27(20):1794–1796.
27. McCaw DL, Pope ER, Payne JT, West MK, Tompson RV, Tate D. Treatment of canine oral squamous cell carcinomas with photodynamic therapy. Br J Cancer 2000;82(7):1297–1299.
28. Allman R, Cowburn P, Mason M. Effect of photodynamic therapy in combination with ionizing radiation on human squamous cell carcinoma cell lines of the head and neck. Br J Cancer 2000;83(5):655–661.
29. Van Geel IP, Oppelaar H, Rijken PF, Bernsen HJ, Hagemeier NE, van der Kogel AJ, Hodgkiss RJ, Stewart FA. Vascular perfusion and hypoxia areas in RIF-1 tumours after photodynamic therapy. Br J Cancer 1996;73(3):288–293.
30. Woodhams JH, Kunz L, Bown SG, MacRobert AJ. Correlation of real-time haemoglobin oxygen saturation monitoring during photodynamic therapy with microvascular effects and tissue necrosis in normal rat liver. Br J Cancer 2004; 91(4):788–794.
31. Gordon ML, Yang VXD, Seng Yue E, Lo S, Wilson BC, Vitkin IA. Doppler optical coherence tomography for monitoring the vascular effects of photodynamic therapy. Proc SPIE 2004; 5316:147–154.
32. Wang HW, Putt ME, Emanuele MJ, Shin DB, Glatstein E, Yodh AG, Busch TM. Treatment-induced changes in tumor oxygenation predict photodynamic therapy outcome. Cancer Res 2004;64:7553–7561.
33. Wiemen TJ, Mang TS, Finger VH, Hill TG, Reed MWR, Corey TS, Nguyen VQ, Render ER. Effect of photodynamic therapy on blood flow in normal and tumor vessels. Surgery 1988;104: 512–517.